

See discussions, stats, and author profiles for this publication at: <https://www.researchgate.net/publication/258377853>

Elastic Nanocomposite Structures Formed by Polyacetylene– Hemicyanine Mixed Films at the Air–Water Interface

ARTICLE *in* THE JOURNAL OF PHYSICAL CHEMISTRY C · NOVEMBER 2013

Impact Factor: 4.77 · DOI: 10.1021/jp406397q

CITATIONS

3

READS

48

5 AUTHORS, INCLUDING:



[Luisa Ariza-Carmona](#)

University of Cordoba (Spain)

3 PUBLICATIONS 3 CITATIONS

SEE PROFILE



[Juan Giner-Casares](#)

CIC biomaGUNE

46 PUBLICATIONS 282 CITATIONS

SEE PROFILE



[Luis Camacho](#)

University of Cordoba (Spain)

150 PUBLICATIONS 1,564 CITATIONS

SEE PROFILE

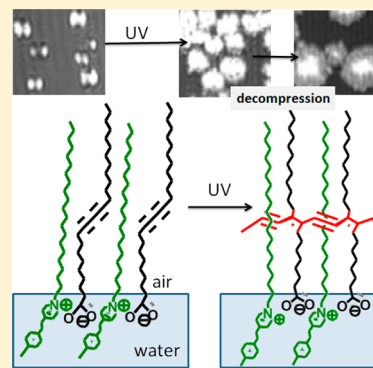
Elastic Nanocomposite Structures Formed by Polyacetylene–Hemicyanine Mixed Films at the Air–Water Interface

Luisa Ariza-Carmona, María T. Martín-Romero, Juan J. Giner-Casares, Marta Pérez-Morales, and Luis Camacho*

Institute of Fine Chemistry and Nanochemistry, Department of Physical Chemistry and Applied Thermodynamics, University of Córdoba, Campus Universitario de Rabanales, Edificio Marie Curie, Córdoba, Spain E-14014

S Supporting Information

ABSTRACT: A mixed film of 10,12-pentacosadiynoic acid (DA) and an amphiphilic cationic hemicyanine (SP) in the ratio 1:1 has been fabricated. This mixed film has been proved to be completely homogeneous due to the good compatibility between both molecules, i.e., hydrophobic regions sized and polar regions of opposite charge. This adequate balance between the vertical sections of the hydrophobic and hydrophilic groups allows the formation of an ion pair between them. In this mixed film, DA molecules organize in monolayer instead of trilayer as occurs for pure DA film. Surface pressure measurements (isotherms and compression–expansion cycles), Brewster angle microscopy, reflection spectroscopy, and PM-IRRAS prove this structure. Using BAM to reveal the structure of this mixed film, circular domains with internal anisotropy because the ordered alignment of hemicyanine groups (strong self-aggregation) are observed. Under UV irradiation a new polyacetylene (PDA) form was fabricated in a homogeneous mixed monolayer despite of the distance measured between the DA molecules by the presence of SP dye. The polymerization takes place only in the circular domains. Under expansion the domains forming during compression and after UV irradiation form a nanocomposite stable material with partially elastic outer region.



■ INTRODUCTION

Polydiacetylenes (PDA) have attracted great attention for application in the sensor field due to their unique colorimetric/fluorescence dual detection capability.^{1–5} In general, diacetylene amphiphilic monomers (DA) are dispersed by sonication in aqueous solution, forming self-assembled liposomes. Alternatively, DA can also be spread at the air–water interface to form Langmuir monolayers and transferred onto a solid substrate via the Langmuir–Blodgett (LB) or Langmuir–Schaefer (LS) film transfer methods to build well-defined self-assembled monolayers^{6–10} or multilayers.^{8,11,12} These well-ordered monomers are then subsequently photopolymerized by UV irradiation. The polymeric backbone formed is composed of alternating double and triple bonds, and the extent of conjugation depends on its conformation.¹³ A conjugated polymer absorbing light at approximately 650 nm gives a blue appearance. However, if the effective conjugation length is reduced by the strain and torsion imposed onto the backbone, the absorption maximum is shifted to about 550 nm and a bright red color is obtained.

The backbone distortion can be induced by order–disorder transitions in the side chains through exposure to heat,^{14–16} organic solvents,^{17,18} pH and salt changes,^{19,20} mechanical stress,^{7,21–23} or, in the case of biosensors, by the specific interaction between a surface bound ligand and its complementary target.^{24–27} In such cases, the colorimetric shift of polydiacetylene lipid systems from blue to red is usually irreversible, and it is a result of a transition from a

thermodynamically metastable blue form to a lower energy red form. To achieve reversible color change, metal ions interactions,^{28,29} nanoparticles interaction,^{30,31} and synthesized diacetylene with different headgroup^{32–36} have been reported. On this basis, PDA has been used as colorimetric sensor; as an example, PDA liposomes are typically modified with a probe, which is complementary of the target, in a way where the target presence is determined by the color change.^{37–39}

Also, the UV light irradiation of the annealed LB films of cadmium diacetylene permits to obtain polydiacetylenes absorbing at 704 nm. This chromatic phase has been designated the bluish-green form.^{14,40,41}

Diacetylene polymerization occurs only when the material is in a highly ordered state and is very sensitive to the surrounding environment.⁴² It requires an optimal packing of the diacetylenic units to allow propagation of the linear chain polymerization through the ordered phase.⁴³ Langmuir monolayer of amphiphilic pentacosadiynoic acid at the air–water interface under a surface pressure of 25 mN/m forms a polymeric blue phase with relatively “expanded” structures where molecules occupy approximately 0.24 nm², while for the red phase the area per molecules is approximately 0.19 nm².⁴⁴

A point of great interest is the study of mixtures of diacetylene amphiphilic monomers and not polymerizable

Received: June 28, 2013

Revised: September 20, 2013

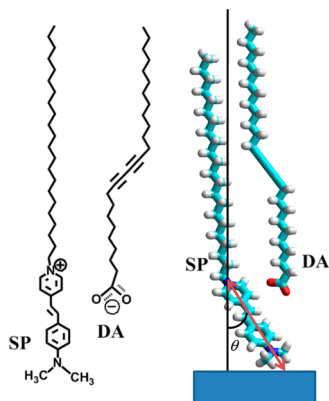
Published: September 24, 2013



lipids.⁴⁵ Under appropriate experimental conditions stable homogeneous systems prior to polymerization can be obtained.^{46–51} However, the polymerization may lead to phase separation and destabilization of the monolayer or bilayer.^{52–54}

In this work, the mixed monolayers formed by 10,12-pentacosadiynoic acid (DA) and an amphiphilic cationic hemicyanine (SP) (their structures are shown in Scheme 1)

Scheme 1. Molecular Structures of SP and DA^a



^aRed arrow indicates the transition dipole moment direction, and θ represents the tilt angle of the hemicyanine group.

in a 1:1 molar ratio (DA:SP = 1:1 monolayers) are studied. Our objective is to analyze whether the DA polymerization is possible in the mixed films and, in the case the polymerization takes place, checking the components' segregation. SP is a dye with good fluorescent properties, while the PDA is widely used as a colorimetric sensor. The initial target is to mix the two components was to test whether the dye could modify the colorimetric properties of the PDA.

For the foregoing reasons and in order to design well-defined structure, where diacetylene polymerization could take place, the lateral organization must be controlled. This control can be achieved by connecting the polar groups, either through hydrogen bonding⁵⁵ via electrostatic interactions or through the self-aggregation of dyes.⁵⁶ Recently, we have used the latter strategy to study mixed films containing dimyristoylphosphatidic acid (DMPA) and an amphiphilic hemicyanine dye (SP) in 1:1 molar ratio⁵⁷ and mixed monolayers of SP and stearic acid (SA) in a 1:1 molar ratio.⁵⁸ For these mixed systems, it has been found that SP forms completely homogeneous monolayers when mixed in a 1:1 ratio with DMPA⁵⁷ or SA.⁵⁸

In the DA:SP = 1:1 monolayers, it is expected that the anionic DA can bind the SP molecule by electrostatic interactions. Additionally, the length of the completely extended SP alkyl chains and the DA length are approximately the same. This dual affinity allows good compatibility between the two molecules resulting in a complete miscibility through both hydrophilic (ion pair) and hydrophobic interactions. Furthermore, it is expected that the small carboxylic acid headgroup of the DA molecule does not avoid the hemicyanine aggregation by the dye molecular tilt. Consequently, the hemicyanine group would have freedom of movement, bending properly to allow its aggregation.

In the resulting mixed monolayer, DA and SP molecules are intercalated so that SP alkyl chains act spacing diacetylene units, which in principle could prevent photopolymerization of

DA. However, it was found that the polymerization takes place without segregation of components. The polymer formed by this method has different properties from those of PDA previously described; i.e., a new PDA form absorbing at 520 nm is obtained. The new form shows a hypochromic shift of 30 nm with respect to the red polymer (550 nm), not fluorescent in this case. Furthermore, under decompression the polymerized mixed monolayer shows domains in which the polymer is expanded, suggesting a certain elasticity degree.

EXPERIMENTAL SECTION

Materials. 10,12-Pentacosadiynoic acid (DA) was purchased from ABCR (Germany) and purified according to the method described elsewhere;^{46,59} that is, the diacetylene monomer was dissolved in chloroform and filtered through a 0.45 μm nylon filter. Purified powder was obtained by evaporation of the solvent.

Hemicyanine dye, 4-[4-(dimethylamino)styryl]-1-docosylpyridinium bromide (SP), was purchased from Sigma-Aldrich and used as received. Their molecular structures are depicted in Scheme 1.

The initial solutions for each component were prepared as well in chloroform. A mixture of trichloromethane and methanol, ratio 3:1 (v/v) was used as cospreading solvent. The pure solvents were obtained without purification from Aldrich (Germany). Ultrapure water, produced by a Millipore Milli-Q unit, pretreated by a Millipore reverse osmosis system ($>18.2 \text{ M}\Omega \text{ cm}$), was used as a subphase. The subphase temperature was 21 $^{\circ}\text{C}$ with pH 5.7.

The substrates used for LB transfer were cleaned as follows: successive steps with an alkaline detergent, isopropanol, and ethanol and then rinsed with ultrapure water.

Isotherms of Langmuir films, Reflection Spectroscopy, and BAM Imaging. Two different models of Nima troughs (Nima Technology, Coventry, England) were used in this work, both provided with a Wilhelmy type dynamometric system using a strip of filter paper: a NIMA 611D with one moving barrier for the measurement of the reflection spectra and a NIMA 601 equipped with two symmetrical barriers to record BAM images. The monolayers were compressed at a speed of $0.03 \text{ nm}^2 \text{ min}^{-1} \text{ molecule}^{-1}$.

For the UV irradiation a UV lamp ($\lambda = 254 \text{ nm}$, $W = 10 \text{ W}$) was mounted on top the trough, keeping a distance of ca. 5 cm from the cospread mixed film prepared at the air–water interface.

UV–vis reflection spectra at normal incidence as the difference in reflectivity (ΔR) of the dye film-covered water surface and the bare surface⁶⁰ were obtained with a Nanofilm surface analysis spectrometer (ref SPEC², supplied by Accurion GmbH, Göttingen, Germany). The reflection spectra were normalized to the same surface density of hemicyanine by multiplying ΔR by the surface area, i.e., $\Delta R_{\text{norm}} = \Delta R \times A$, where A ($\text{nm}^2/\text{molecule}$) is taken from the surface pressure–area (π – A) isotherms.

Images of the film morphology were obtained by Brewster angle microscopy (BAM) with a I-Elli2000 (Accurion GmbH) using a Nd:YAG diode laser with wavelength 532 nm and 50 mW, which can be recorded with a lateral resolution of 2 μm . The image processing procedure included a geometrical correction of the image as well as a filtering operation to reduce interference fringes and noise. The microscope and the film balance were located on a table with vibration isolation

(antivibration system MOD-2 S, Accurion, Göttingen, Germany) in a large class 100 clean room.

PM-IRRAS spectra were recorded using a KSV PMI 550 (KSV NIMA, Espoo, Finland) equipped with an MCT detector. A detailed description of the PM-IRRAS setup and the experimental procedure has already been given elsewhere.⁶¹ The angle of incidence of the infrared beam with respect to the surface normal was 75°. PM-IRRAS spectra were recorded with a spectral resolution of 8 cm⁻¹ and collected using 3000–6000 scans for 5–15 min.

Langmuir–Blodgett Films. The monolayers were transferred onto quartz substrates. The mixed monolayers were transferred by the Langmuir–Blodgett, i.e., by vertical dipping at constant surface pressure with the lifting speed of 5 mm min⁻¹. The multilayers were assembled by sequential monolayer transfer. The transfer ratio was close to unity for all transfer processes. UV–vis electronic absorption spectra of the films were measured locating the substrate directly in the light path on a Cary 100 Bio UV–vis spectrophotometer. The steady state fluorescence and excitation spectra were measured using a FS920 steady state fluorimeter (Edinburgh Instrument, Livingston, UK).

RESULTS AND DISCUSSION

Surface Pressure–Area Isotherms. Mixed monolayers of DA:SP = 1:1 have been prepared at the air–water interface by the cospreading method.^{62,63} Figure 1 (red line) shows the

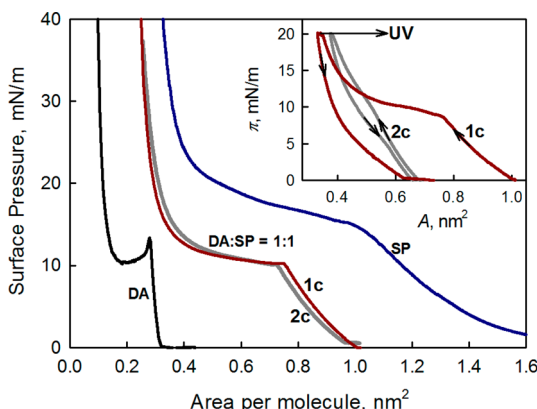


Figure 1. Surface pressure–area (π – A) isotherms of DA (black line), SP (blue line), and first (red line) and second (gray line) compression processes of a mixed DA:SP = 1:1 monolayer. Inset: effect of UV radiation on the mixed film.

surface pressure–area (π – A) isotherm of the mixed DA:SP monolayer. The takeoff of the isotherm occurs at 1.0 nm²/molecule, and the isotherm shows a phase transition at ~9.5 mN/m and ~0.75 nm²/molecule. For comparison, Figure 1 also shows the pure DA (black line) and SP (blue line) isotherms. Isotherms of pure components are coincident with those published previously.^{12,64–66}

DA monolayer on pure water subphase collapses when the area decreases below 0.25 nm²/molecule, forming a trilayer (for example in Figure 1, black line, π = 40 mN/m, A = 0.1 nm²/molecule), as previously described.^{12,66} However, for the mixed monolayer at π = 40 mN/m, the area per molecule is ~0.25 nm², intermediate value between the area occupied per SP molecule (~0.33 nm²)⁶⁷ and that of the alkyl chain with completely vertical orientation (~0.20 nm²). This behavior

indicates that the trilayer is not formed in the mixed monolayer, at least below π = 40 mN/m.

Successive compression–expansion cycles were recorded to study the homogeneity of the mixed film. In Figure 1, first and second compression cycles are indicated by 1c (red line) and 2c (gray line), respectively. The area hysteresis between the both cycles is always less than 5%.

The effect of UV radiation on the mixed monolayer is also shown in Figure 1, inset. The procedure was the following: the mixed monolayer was compressed up to 20 mN/m, and under constant surface pressure the film was irradiated for 8 min. Throughout that time the surface area per molecule decreases from 0.35 to 0.33 nm². After the irradiation the monolayer was expanded, and finally a second compression–decompression cycle (gray line) was done. The UV irradiation process shrinks the monolayer at low surface pressures (below 12 mN/m) and expands it at high surface pressure (above 12 mN/m).

In a previous work, we have demonstrated that SP, a cationic amphiphilic molecule (see Scheme 1), forms homogeneous mixed monolayers with anionic amphiphilic molecules such as DMPA⁵⁷ and SA⁵⁸ in a 1:1 molar ratio. Those mixed films showed of great stability as a result of charge compensation and the compatibility of the alkyl chains of the two components, which favors the complete miscibility of the mixture. The results shown below confirm the complete miscibility of the mixed DA:SP = 1:1 monolayers. Therefore, in this work we have studied exclusively the equimolar DA:SP mixture.

Brewster Angle Microscopy (BAM). Simultaneously to the isotherm recording, the morphology of the mixed monolayer at the air–water interface is directly observed by BAM. For π < 9 mN/m, below the phase transition, the mixed monolayer appears to be homogeneous (images not shown), indicating the complete miscibility of the components. For π ≈ 9 mN/m small circular domains emerge (Figure 2a, π = 10 mN/m). These circular domains are related to the phase transition observed in the isotherm (see Figure 1), having inner textures with different brightness, i.e., the circle regions located above and below are darker than their surrounding area, while the lateral regions of the circle are brighter.

The shape and texture of these domains (Figure 2a) are similar to that observed in referenced above mixed monolayers containing SP and anionic amphiphilic as DMPA⁵⁷ or SA⁵⁸ in the ratio 1:1. For those mentioned systems the domain shape is determined both by the strong tendency to self-aggregation hemicyanine polar group and the available area under the alkyl chains for this self-aggregation. Moreover, the texture of the domain does not depend on the packing of alkyl chains but on the rearrangement of the hemicyanine group, because this group absorbs at the laser wavelength used in BAM.⁶⁸ Domains anisotropy results from the molecular alignment of the group hemicyanine due to the strong tendency to self-aggregation of this group.

The BAM images of the mixed monolayer does not show the typical dendritic structure observed for pure DA monolayers.^{66,69,70} The absence of these structures is an additional evidence of the complete miscibility of that SP and DA in a 1:1 ratio and forming an ion pair.

Under increasing surface pressure (Figure 2b, π = 20 mN/m), the domains grow and the texture inside the domain is similar to that observed at lower surface pressure. However, the periphery of the domain has a gray hedge, indicating that in this region there is not anisotropy, and therefore there is no a good molecular alignment of the hemicyanine group. That the

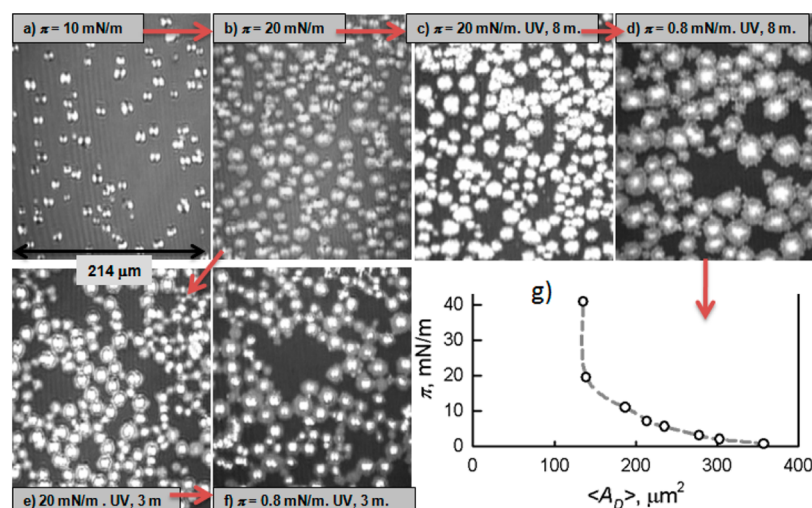


Figure 2. BAM images of the mixed DA:SP = 1:1 monolayer before the polymerization: (a) $\pi = 10$ mN/m and (b) $\pi = 20$ mN/m; after 8 min of polymerization, (c) $\pi = 20$ mN/m, and (d) $\pi = 0.8$ mN/m (expansion cycle); after 3 min of polymerization, (e) $\pi = 20$ mN/m and (f) $\pi = 0.8$ mN/m (expansion cycle). (g) Plot of the π vs $\langle A_D \rangle$. The domain average area was obtained by compressing the monolayer once reached conditions as in (d).

domains have different texture inside and in its periphery does not mean that the composition is different in these regions. In our case, what we can visualize in BAM is the alignment of the hemicyanine groups.⁶⁸ Therefore, the gray region only can be interpreted as a loss of the existing order respect to the domain core. At high surface pressure ($\pi = 40$ mN/m), the surface is completely covered by domains (images not shown), the area per molecule being ~ 0.25 nm². This area value is related to the area occupied per molecule inside the domain as discussed below.

Figure 2c shows a BAM image at $\pi = 20$ mN/m, after the UV irradiation for 8 min. The shape of the domains does not change after irradiation, although the domains obtained are brighter, so that the internal texture disappears. As demonstrated below, during irradiation process the polymer is formed, and the polymer has its maximum absorption at 520 nm, very close to the laser wavelength used in BAM (532 nm). The absorption of radiation causes a sharp increase in the reflection, which is detected by BAM. Another significant fact is that during the irradiation process the monolayer area almost not change (decreases slightly from $A = 0.35$ to 0.33 nm²). At this point, it is necessary to emphasize that the domain surrounding regions do not increase the brightness. This feature evidences that the polymerization takes place exclusively within the domains, in both its internal and periphery region.

The BAM image in Figure 2d shows expanded monolayer after the polymerization. The bright domains expand but not disappear. This phenomenon is noteworthy in comparison with the monolayer under compression at $\pi = 20$ mN/m (Figure 2b) without UV irradiation and subsequently expanded where the domains disappear (data not shown). The persistence of the domains for the mixed film after irradiation and subsequent decompression is an evidence of the PDA polymerization and that the polymerization takes place only inside the domains. The latter has been tested by radiating at different surface pressures where different degrees of growth of the domains are detected. In all cases, the polymerization takes place exclusively inside the domain.

The expanded polymeric domains (Figure 2d) show a striking texture with a bright central region and a periphery less

bright. Furthermore, the average size of the domains is higher than a high pressure surface (Figure 2c), indicating its elastic character. This elastic property has not previously been observed in polyacetylene materials. Furthermore, this elasticity is not the same inside than in the periphery region of the domain. In order to quantify this phenomenon, the surface compressional modulus, also called static elastic modulus, $\kappa = -A(d\pi/dA)$, of the mixed monolayer before and after polymerization at 20 mN/m for 8 min has been calculated (see Figure S1B in the Supporting Information). With respect to the polymerized film, κ display a maximum ($\kappa \approx 40$ mN/m) for $A = 0.55$ nm² ($\pi \approx 7.5$ mN/m). This value is an average which refers not only to the domains but also at the monolayer region where polymerization did not take place. However, for unpolymerized monolayer $\kappa \approx 6$ mN/m at $A = 0.55$ nm² (see Figure S1), so the value of $\kappa \approx 40$ mN/m should be attributed largely to the domains observed.

Different BAM images of the polymerized monolayer at different surface pressures are shown in Figure S2. These images correspond to the second compression cycle after polymerization (see inset in Figure 1, line gray). From these BAM images the domain average area, $\langle A_D \rangle$, can be obtained. Such a value was estimated from the area fraction occupied by domains and the number of domains in each BAM image. The experiment was repeated three times to obtain the average value for some surface pressures. In Figure 2g, the plot of the π vs $\langle A_D \rangle$ is shown. For the surface pressure range between 3 and 11 mN/m, $\langle A_D \rangle$ varies in an approximately linear way, which permits us to estimate that for $\pi \approx 7.5$ mN/m $\kappa \approx 25$ mN/m. Also, in the figure and for $\pi > 20$ mN/m, $\langle A_D \rangle$ is constant, indicating that the domains reaches a rigid state ($\kappa \rightarrow \infty$).

The κ value could be correlated with the monolayer physical state.⁷¹ Namely, the values of κ below 100 mN/m correspond to the liquid expanded state, ranging from 100 to 250 mN/m to the liquid condensed state and greater than 250 mN/m to the solid state of the monomolecular film. For $\pi < 20$ mN/m, the PDA:SP domains possess static elastic modulus in the range to those found in the expanded liquid phase, which indicates its elastic character.

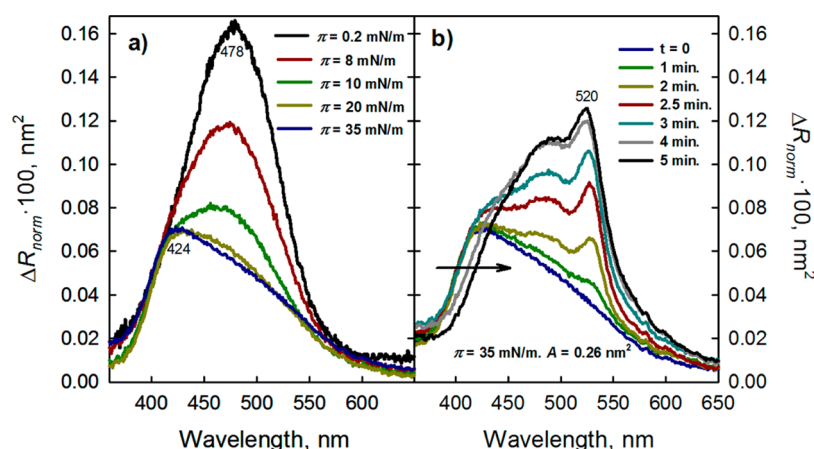


Figure 3. (a) Normalized reflection spectra of the mixed DA:SP = 1:1 monolayer at different surface pressures. (b) Normalized reflection spectra of the mixed film as a function of the UV irradiation time.

To determine the time effect on the polymerization process, BAM images of the mixed film compressed at $\pi = 20$ mN/m after UV irradiation during 3 min were registered (Figure 2e). For this period of time, the polymerization does not take place completely, as discussed below. In this case (Figure 2e), we can observe domains in which there is a very bright central region that retains the shape of the anisotropy region observed in Figure 2a and a slightly brighter outer halo. Under decompression the mixed-polymerized monolayer (Figure 2f) shows domains with a central region similar to that observed in Figure 2d (UV irradiation for 8 min), while the peripheral region has less brightness than in the previous case. This behavior indicates (1) the molecular organization should not be the same in the central region than in the periphery of the domain and (2) the organization influences on the density and the degree of polymerization. Most likely, the polymer density should be lower in the peripheral region, which provides it some elasticity. Finally, the phenomenon observed here (Figure 2d,f) is reversible, so that under a new compression process, the mixed-polymerized monolayer, the domains as those shown in Figure 2c,e are obtained.

Reflection Spectroscopy at the Air–Water Interface.

Reflection spectroscopy at the air–water interface detects only those molecules which are at the interface and contribute to enhanced reflection from the air–water interface.⁶⁰ This technique gives us valuable information on the organization, density, and orientation of the chromophore molecules located at the air–water interface.⁷² For low values of absorption, the reflection, ΔR , has been shown to be proportional to the surface concentration of the chromophore. It is usual to represent the reflection spectra as product $\Delta R \times A = \Delta R_{\text{norm}}$, whose magnitude represents the reflection normalized to the molecular surface density.⁷² ΔR_{norm} must remain invariant throughout the compression process if any changes in the chromophore orientation or aggregation phenomena happen. Therefore, a ΔR_{norm} plot shows more clearly the changes of orientation and/or association than the directly measured spectra.^{57,72}

Figure 3a displays the normalized reflection spectra of the DA:SP 1:1 film before polymerization. At low surface pressures ($\pi < 10$ mN/m), the spectra present a band at 478 nm. As the surface pressure increases the following is appreciated: ΔR_{norm} decreases and the maximum wavelength of the band shifts to shorter wavelengths (from 478 to 424 nm). Both phenomena

are related to the decreasing of the tilt angle of the hemicyanine group (see θ in Scheme 1)⁷² and the formation of H aggregates of the hemicyanine chromophores,^{57,65,73–75} respectively. The behavior described in Figure 3a is very similar to that observed in the mixed monolayers containing SP and DMPA⁵⁷ or SA⁵⁸ and will not be discussed in greater depth here. However, it is noteworthy the maximum ΔR_{norm} values achieved in Figure 3a are about half those obtained for the mixed monolayers with DMPA⁵⁷ or SA.⁵⁸ In such cases, the reflection was normalized with respect to the area per SP molecule, while in this work ΔR is normalized with respect to the area per total molecule.

Keeping a constant surface pressure of $\pi = 35$ mN/m, the mixed monolayer was irradiated with UV light and the reflection spectra were recorded as a function of time (Figure 3b). As the time irradiation increases, the reflection signal increases and a new peak at 520 nm and a shoulder at 490 nm appear. These peaks must be related to the formation of polymer and the increase of the reflection signal to the origin of the increased brightness in the domains observed in BAM (see Figure 2, being $\lambda_{\text{laser-BAM}} = 532$ nm). Another significant fact derived from the reflection measurement is that the hemicyanine band shifts to longer wavelengths, which should be related to the partial disaggregation of this group, see black arrow in Figure 3b.

Polymerizing pure DA monolayers initially leads to the formation of the blue form of the polymer, with the main absorption band at 650 nm. Prolonged application of UV radiation,⁷⁶ or monolayer compression,⁷⁷ transforms the blue polymer to the red form ($\lambda_{\text{max}} = 550$ nm). However, this behavior has not been observed in the mixed PDA:SP monolayer, where a polymer with absorption band at 520 nm has been formed.

The stability of the polymerized system has been also followed by UV–vis reflection spectroscopy. Figure 4a shows some normalized reflection spectra obtained during the decompression process, after polymerization of the mixed film. ΔR_{norm} keeps a constant value in the region of large wavelengths, above 520 nm, which indicates that the polymer does not change its orientation with respect to the interface. However, in the region of short wavelengths where the hemicyanine group absorbs, an increase of reflection is obtained. This behavior can be interpreted as due to a change of the inclination of the hemicyanine group as the surface

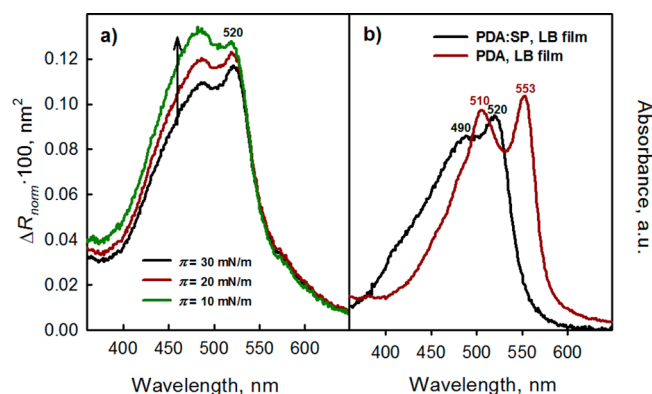


Figure 4. (a) Normalized reflection spectra of the polymerized mixed monolayer, PDA:SP = 1:1, at different surface pressures. (b) Absorption spectra of a polymerized mixed LB-film, PDA:SP = 1:1 (black line), and a polymerized pure DA monolayer (red line) as a reference. $\pi_{\text{transfer}} = 35 \text{ mN/m}$.

pressure increases (increase of θ angle, see Scheme 1), just the opposite of the phenomenon described for Figure 3a.

Transmission Spectroscopy of DA:SP = 1:1 LB Films.

Langmuir mixed monolayers of DA:SP = 1:1 have been transferred onto quartz supports at constant surface pressures, $\pi_{\text{trans}} = 35 \text{ mN/m}$, by using the LB method with transfer ratios close to unity in all cases. To prove the effect of the UV irradiation on the organization of the Langmuir and Langmuir–Blodgett films, two different samples were fabricated: (i) one mixed DA:SP film was prepared at the air–water interface, irradiated for 8 min, and finally transferred by LB method at 35 mN/m to the solid support; (ii) one mixed DA:SP 1:1 monolayer was transferred at 35 mN/m and then irradiated for 8 min. The absorption spectra for both samples were almost identical (see Figure 4b, black line).

Diacetylene polymerization leads to two different colorimetric conformations: the blue form absorbing light at approximately 650 nm and the red form with the absorption maximum about 550 nm. As a reference, one LB film of pure PDA was prepared showing the typical spectrum of this material when polymerized to the red form (Figure 4b, red line). It is clearly appreciated the position of the absorption bands for the red polymer (553 nm) does not match those registered for the polymer in the mixed films (520 nm). The organization by the polymerization process in the mixed monolayer shifts the maximum to shorter wavelengths with respect to that described for the pure PDA. Therefore, the presence of SP in the mixed monolayer disturbs DA polymerization, resulting in a type of polymer in which the conjugation of double and triple bonds is different to that existing in the red or blue forms of the polymer described elsewhere.⁷

Transmission spectra of the LB films have been obtained under 45° incidence angle, with s- and p-polarized light to determine the organization for the SP and PDA molecules in the mixed film. Figure 5 shows the s and p spectra for one mixed monolayer transferred at $\pi_{\text{trans}} = 35 \text{ mN/m}$, before (Figure 5a) and after (Figure 5b) the UV polymerization. To discard the anisotropy in the plane of the quartz substrate, at least on the area covered by the footprint of the incident light beam, spectra were recorded under normal incidence of light at different polarization angles. The obtained spectra were identical in all cases.

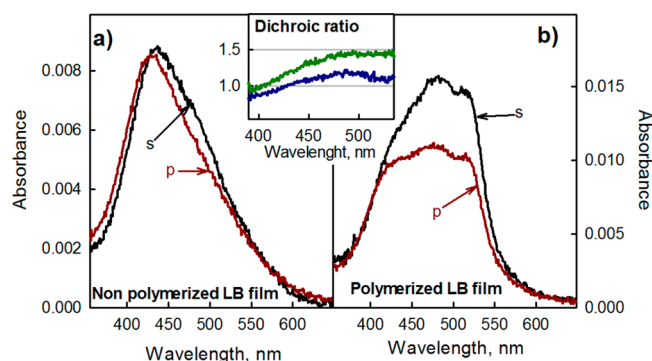


Figure 5. Absorption spectra under 45° incidence angle of (a) LB film of DA:SP 1:1 with s-polarized light (black line) and p-polarized light (red line) and (b) LB film of PDA:SP 1:1 with s-polarized light (black line) and p-polarized light (red line). Inset: dichroic ratio for DA:SP 1:1 (blue line) and for PDA:SP 1:1 (green line).

Figure 5a shows the transmission spectra before the polymerization under 45° of incidence and s (black line) and p (red line) polarized light. The spectra under s- and p-polarized shift the absorption maximum from 436 nm (s-spectrum) to 428 nm (p-spectrum). However, at the air–water interface the absorption maximum under normal incidence was located at 424 nm (Figure 3a).

Note that the polarized spectra cross-link, so that for wavelengths above the absorption maximum the s-spectrum is more intense than the p-spectrum, while the opposite occurs at wavelengths lower than the absorption maximum.

These spectroscopic results can be interpreted by using the dichroic ratio, $DR = A_{\text{s}}/A_{\text{p}}$ (see Figure 5, inset). Thus, for an incidence angle of 45° and before the polymerization (blue line), the DR ratio varied from ~0.88 at $\lambda = 400 \text{ nm}$ to ~1.15 at $\lambda = 500 \text{ nm}$. This behavior has been interpreted due to the splitting of the absorption band of the hemicyanine. This phenomenon is similar to that observed in the case of the SP:SA system⁵⁸ and because of the existence of inequivalent molecules in the hemicyanine aggregate. According to Davidov's exciton theory, a given molecular energy level may be split into as many components as there are inequivalent molecules per unit cell.^{78,79} In addition to the spectral splitting, the Davydov bands exhibit distinct polarization properties, as in our case. Following a procedure identical to that used for the system SP:SA,⁵⁸ the average tilt angle of the hemicyanine transition dipole with respect to the normal of the support has been determined to be $\theta \approx 34^\circ$.

In Figure 5b, the s- and p-spectra of the mixed film after polymerization are shown. In this case, the s-spectrum is always more intense than the p-spectrum. The dichroic ratio is also shown in Figure 5, inset, green line. As described before, the DR changed along the absorption band, showing in the region of hemicyanine absorption a value close to that obtained before the polymerization, and near to the polymer absorption maximum (520 nm), a value $DR \sim 1.5$. This DR value can be related to an orientation of the polymer absorption component almost parallel to the support.⁵⁸

Since it is not possible to resolve qualitatively absorption bands of the polymer and hemicyanine, it can be estimated that the polymer absorption component (conjugated double and triple bonds) is parallel to the support, while the hemicyanine absorption component at surface pressure constant hardly

changes its orientation after polymerization, although its aggregation changes as discussed above.

The domains anisotropy observed by BAM before polymerization is the result of the orderly alignment of the hemicyanine groups originated by its strong self-aggregation. However, after polymerization, the domain's anisotropy disappears, indicating that the conjugated polymer chains are not aligned along a preferential direction within the domain. The polymerization also seems to influence the aggregation of the hemicyanine molecules and thus their alignment involving the loss of hemicyanine order.

Finally, fluorescence measurements of the LB mixed films have been done. Before polymerization, the mixed LB film is fluorescent which emission band corresponds to the hemicyanine group ($\lambda_{\text{emission}}$ at ~ 590 nm). However, after polymerization, the mixed LB PDA:SP film does not fluoresce. This fact indicates a complete energy transfer between hemicyanine and polymer and that the polymer formed in this mixed film is not fluorescent, unlike the red polymer form (absorption band at 550 nm), which is fluorescent.^{80,81}

PM-IRRAS Measurements. Figure 6 shows the PM-IRRAS spectrum of the mixed monolayer DA:SP = 1:1 after the

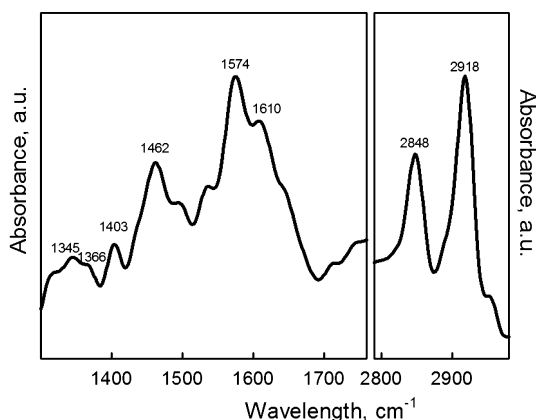


Figure 6. PM-IRRAS spectrum of the mixed monolayer PDA:SP = 1:1 (UV irradiation for 8 min) at the air–water interface at 30 mN/m.

polymerization (UV irradiation for 8 min) at the air–water interface at 30 mN/m. The asymmetric and symmetric stretching mode of methylene groups from the alkyl chains, $\nu_{\text{as}}(\text{CH}_2)$, at 2920 cm^{-1} , and $\nu_{\text{s}}(\text{CH}_2)$, at 2850 cm^{-1} , are clearly distinguishable. Previous IR studies have shown that the location of $\nu_{\text{as}}(\text{CH}_2)$ and $\nu_{\text{s}}(\text{CH}_2)$ modes are sensitive indicators for the lateral interactions between alkyl chains.^{82–86}

Thus, the band position for the $\nu_{\text{as}}(\text{CH}_2)$ mode is 8 cm^{-1} lower in the crystalline state (2920 cm^{-1}) than that for the liquid state (2928 cm^{-1}), whereas for the $\nu_{\text{s}}(\text{CH}_2)$ mode the band position is 6 cm^{-1} lower in the crystalline sample (2850 cm^{-1}) than in the liquid (2856 cm^{-1}).^{86,87} The low wavenumbers observed for the $\nu_{\text{as}}(\text{CH}_2)$ and $\nu_{\text{s}}(\text{CH}_2)$ modes are indicative of a tightly packing of the hydrocarbon chains.

In the spectrum can also be observed two intense bands at 1574 and 1462 cm^{-1} , which may be related to the asymmetric and symmetric modes of the COO^- group, respectively.^{88,89} From these results the absence of bands in the $1740\text{--}1680\text{ cm}^{-1}$ region proves a significant fact. In this region, the carbonyl stretching (with or without hydrogen bond) of undissociated carboxyl acid group must be observed.^{88–90} The absence of such bands is an evidence that the carboxyl group is

completely dissociated, even at the surface pressure of 30 mN/m, which agrees with the formation of ion pair between DA and SP.

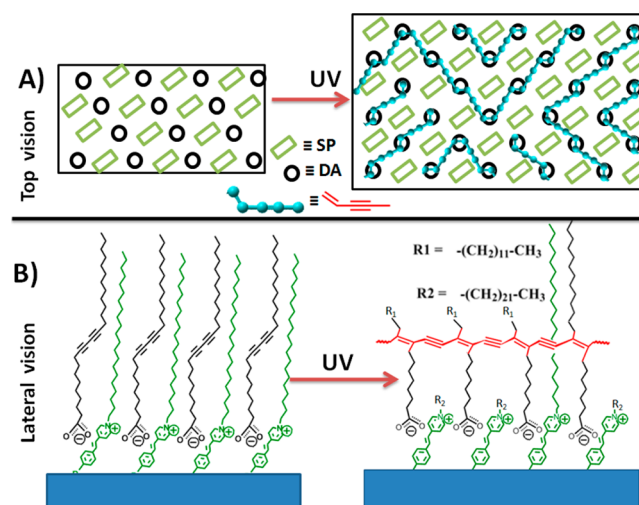
In the spectrum other bands of lesser intensity, such as 1345 cm^{-1} (phenyl), 1366 cm^{-1} ($\delta(\text{CH}_3)$), 1403 cm^{-1} ($\delta(\text{CH}_2)$), and 1610 cm^{-1} (phenyl or $\delta(\text{CN})$ ring stretch), can be observed.

CONCLUSIONS

In this work the mixed monolayer containing SP and DA in a 1:1 ratio has been studied. The mixture has been proved to be completely homogeneous due to the good compatibility between both molecules, that is, hydrophobic regions sized and polar regions of opposite charge. This proper balance between the vertical sections of the hydrophobic and hydrophilic groups allows the formation of an ion pair between them. Evidence of this formation is obtained from the π –A isotherm showing no formation of trilayer, as characteristic from the isotherm of pure DA film^{12,66} and also indicating the components of the mixture do not segregate. Moreover, by BAM the typical dendritic structures observed for pure DA films are not detected.^{66,69,70} However, circular domains with internal anisotropy, similar to those observed in different 1:1 mixed monolayers formed by SP and anionic amphiphilic as DMPA⁵⁷ or SA,⁵⁸ were registered. Finally, the completely dissociated state of the carboxylic group of DA molecules is detected by PM-IRRAS and points to the formation of ion pair between the DA anionic carboxylic group and the hemicyanine group positively charged.

Before the polymerization, domain internal anisotropy must be related to ordered alignment hemicyanine group, owing to its strong self-aggregation.⁵⁷ UV–vis reflection spectroscopy at the air–water interface shows how as surface area decreases, the hemicyanine tilt angle decreases up to a minimum angle close to 34° . Additionally these UV–vis reflection spectra prove the H-type aggregation of the hemicyanine group. An idealized sketch of the internal structure of the domains is shown in Scheme 2 (left, from a top (A) and lateral (B) perspective). In

Scheme 2. Idealized Scheme Displaying the Photopolymerization of the Mixed DA:SP = 1:1 Monolayer where the Alkyl Chains of the SP Molecules Remain Inserted between Polydiacetylene Segments: (A) Top Vision, (B) Lateral Vision



this representation it is assumed that SP and DA form orthorhombic two-dimensional network, such as in the case of mixed films SP:SA.⁵⁸ As was mentioned, when the domain grows (Figure 2b), its outermost region shows a gray texture. This change in texture only can be interpreted as a loss of ordering of hemicyanine groups. We think that in domain periphery region the anisotropy disappears, possibly because of the existence of a large number of lattice defects (loss of order). But the two-dimensional network is formed since the domain continues to grow.

Inside the domains the area per molecule is $\sim 0.25 \text{ nm}^2$, i.e., $\sim 0.5 \text{ nm}^2$ per DA molecule. Despite this great separation between DA molecules, the photopolymerization under UV irradiation takes place without segregation of components, which indicates a highly ordered state and an adequate packing of the diacetylene units.⁴³ That is, the alkyl chains of the SP molecules remain inserted between polydiacetylene segments, forming a highly ordered composite material. Furthermore, after polymerization, the domain anisotropy disappears, indicating that the conjugated polymer chains are not aligned along a preferential direction within the domain. An idealized sketch after the polymerization is shown in Scheme 2 (right, (A) from a top and (B) lateral perspective). In this scheme the polymer chains are intercalated, proposing that the conformation of linear polymer chains can change. In this way, the polymeric structure forms a mesh which makes the domain hold together (but elastically) when it is decompressed. This meshlike structure without a preferred orientation of the PDA absorbing component would explain the disappearance of domain anisotropy after polymerization. Moreover, in an orthorhombic structure the spacing between adjacent molecules is not equivalent. Therefore, for the polymerization taking place in any direction, such a structure must be altered. An experimental evidence of this fact is the change in the hemicyanine aggregation observed after polymerization by means of reflection spectroscopy.

In the formed polymer, the conjugation between the double and triple bonds seems altered as a result of distortion caused by the SP alkyl chains, obtaining a PDA material with different properties than those previously described for the red and blue forms of polyacetylene. Thus, blue and red polymer forms have absorption maxima at ~ 650 and ~ 550 nm, respectively, although for the system investigated here the absorption maximum occurs at ~ 520 nm, i.e., 30 nm blue-shift with respect to the red polymer form. Moreover, the PDA material in the mixed PDA:SP 1:1 monolayer does emit fluorescence, as opposite to the fluorescence of the red polymer form. In fact, the mixed films are fluorescent before the polymerization because of the hemicyanine emission. However, after the polymerization by UV irradiation the mixed film does not show any fluorescent emission, meaning that the polymer is not fluorescent and a complete energy transfer between hemicyanine and polymer happens.

The main evidence that the SP:DA mixture is completely homogeneous is that after polymerization the polymer absorption peak appears at 520 nm exclusively. Segregation of the components should result in polymer shapes with absorption bands at 550 and 650 nm. This has been verified experimentally. Thus, preliminary experiments have been carried out at acidic pH subphase, where DA molecules are undissociated. In these cases, and after UV polymerization, we observed the formation of the blue (650 nm) and the red

polymer (550 nm), although the formation of the polymer at 520 nm was not detected.

In the literature, it has been described as polymerized DA vesicles in neutral pH aqueous solution and with absorbance maximum at 540 nm, after the addition of cetyltrimethylammonium bromide (CTAB), shift the absorbance maximum at 510 nm,^{91,92} a wavelength close to that observed by us after polymerization of the mixed film. The authors propose that as CTAB molecule has a long alkyl chain, hydrophobic interaction would drive the alkyl chain to incorporate with the hydrophobic domain of the vesicle.⁹¹

Noteworthy, the polymerization takes only place in the circular domains. The absence of polymerization in the surrounding regions of the domains should be related to the lower molecular density in those regions and therefore to an inadequate packing of diacetylene units. Finally, monolayer decompression does not imply the disappearance of polymerized domains; on the contrary, these domains form a nanocomposite stable material, partially elastic in its outer region.

■ ASSOCIATED CONTENT

● Supporting Information

Surface pressure–area isotherms and static elastic modulus of the mixed monolayer DA:SP = 1:1; BAM images of the mixed monolayer after the polymerization during a second compression process; complete references with more than 10 authors. This material is available free of charge via the Internet at <http://pubs.acs.org>.

■ AUTHOR INFORMATION

Corresponding Author

*Tel +034 957218617; e-mail qf1cadel@uco.es (L.C.).

Notes

The authors declare no competing financial interest.

■ ACKNOWLEDGMENTS

The authors thank the Spanish CICYT for financial support of this research in the Framework of Project CTQ2010-17481 (FEDER A) and also thank Junta de Andalucía (Consejería de Economía, Innovación, Ciencia y Empleo) for special financial support (P08-FQM-4011). Luisa M^a Ariza-Carmona thanks the Ministerio de Economía y Competitividad for her predoctoral grant (Formación de Personal Investigador, FPI).

■ REFERENCES

- (1) Sun, X. M.; Chen, T.; Huang, S. Q.; Li, L.; Peng, H. S. Chromatic Polydiacetylene with Novel Sensitivity. *Chem. Soc. Rev.* **2010**, *39*, 4244–4257.
- (2) Lee, J.; Yarimaga, O.; Lee, C. H.; Choi, Y. K.; Kim, J. M. Network Polydiacetylene Films: Preparation, Patterning and Sensor Applications. *Adv. Funct. Mater.* **2011**, *21*, 1032–1039.
- (3) Yoon, B.; Ham, D. Y.; Yarimaga, O.; An, H.; Lee, C. W.; Kim, J. M. Inkjet Printing of Conjugated Polymer Precursors on Paper Substrates for Colorimetric Sensing and Flexible Electrothermochromic Display. *Adv. Mater.* **2011**, *23*, 5492–5497.
- (4) Lee, J.; Seo, S.; Kim, J. Colorimetric Detection of Warfare Gases by Polydiacetylenes Toward Equipment-Free Detection. *Adv. Funct. Mater.* **2012**, *22*, 1632–1638.
- (5) Zhu, C. L.; Liu, L. B.; Yang, Q.; Lv, F. T.; Wang, S. Water-Soluble Conjugated Polymers for Imaging, Diagnosis, and Therapy. *Chem. Rev.* **2012**, *112*, 4687–4735.

- (6) Day, D.; Ringsdorf, H. Polymerization of Diacetylene Carbonic-Acid Monolayers at Gas-Water Interface. *J. Polym. Sci., Part C: Polym. Lett.* **1978**, *16*, 205–210.
- (7) Tomioka, Y.; Tanaka, N.; Imazeki, S. Surface-Pressure-Induced Reversible Color-Change of a Polydiacetylene Monolayer at a Gas Water Interface. *J. Chem. Phys.* **1989**, *91*, 5694–5700.
- (8) Tieke, B.; Lieser, G.; Wegner, G. Polymerization of Diacetylenes In Multilayers. *J. Polym. Sci., Part A: Polym. Chem.* **1979**, *17*, 1631–1644.
- (9) Zhou, H. L.; Lu, W. X.; Yu, S. F.; He, P. S. Polymerization of 10,12-Pentacosadiynoic Acid Monolayer at Varying Surface Pressure and Temperature. *Langmuir* **2000**, *16*, 2797–2801.
- (10) Friedman, S.; Kolusheva, S.; Volinsky, R.; Zeiri, L.; Schrader, T.; Jelinek, R. Lipid/Polydiacetylene Films for Colorimetric Protein Surface-Charge Analysis. *Anal. Chem.* **2008**, *80*, 7804–7811.
- (11) Tieke, B.; Bloor, D. Raman-Spectroscopic Studies of the Solid-State Polymerization of Diacetylenes. 3. UV-Polymerization of Diacetylene Langmuir-Blodgett Multilayers. *Makromol. Chem., Macromol. Chem. Phys.* **1979**, *180*, 2275–2278.
- (12) Sasaki, D. Y.; Carpick, R. W.; Burns, A. R. High Molecular Orientation in Mono- and Trilayer Polydiacetylene Films Imaged by Atomic Force Microscopy. *J. Colloid Interface Sci.* **2000**, *229*, 490–496.
- (13) Tanaka, H.; Gomez, M. A.; Tonelli, A. E.; Thakur, M. Thermochromic Phase-Transition of a Polydiacetylene, Poly(Etcd), Studied by High-Resolution Solid-State C-13 NMR. *Macromolecules* **1989**, *22*, 1208–1215.
- (14) Shibata, M.; Kaneko, F.; Aketagawa, M.; Kobayashi, S. Reversible Color Phase-Transitions and Annealing Properties of Langmuir-Blodgett Polydiacetylene Films. *Thin Solid Films* **1989**, *179*, 433–437.
- (15) Patel, G. N.; Witt, J. D.; Khanna, Y. P. Thermochromism in Polydiacetylene Solutions. *J. Polym. Sci., Part B: Polym. Phys.* **1980**, *18*, 1383–1391.
- (16) Exarhos, G. J.; Risen, W. M.; Baughman, R. H. Resonance Raman Study of Thermochromic Phase-Transition of a Polydiacetylene. *J. Am. Chem. Soc.* **1976**, *98*, 481–487.
- (17) Chu, B.; Xu, R. L. Chromatic Transition of Polydiacetylene in Solution. *Acc. Chem. Res.* **1991**, *24*, 384–389.
- (18) Chance, R. R. Chromism in Polydiacetylene Solutions and Crystals. *Macromolecules* **1980**, *13*, 396–398.
- (19) Cheng, Q.; Stevens, R. C. Charge-Induced Chromatic Transition of Amino Acid-Derivatized Polydiacetylene Liposomes. *Langmuir* **1998**, *14*, 1974–1976.
- (20) Aghatabay, N. M.; Lindsell, W. E.; Preston, P. N.; Tomb, P. J. Synthesis and Characterization of Carboxylic-Acid and Diphenylphosphine Derivatives in the 1,3-Diyne Series - Spectral Properties of Polydiacetylene Carboxylates. *Polym. Int.* **1993**, *31*, 367–374.
- (21) Tashiro, K.; Nishimura, H.; Kobayashi, M. First Success in Direct Analysis of Microscopic Deformation Mechanism of Polydiacetylene Single Crystal by the X-Ray Imaging-Plate System. *Macromolecules* **1996**, *29*, 8188–8196.
- (22) Tanaka, H.; Thakur, M.; Gomez, M. A.; Tonelli, A. E. Study of the Thermochromic Phase-Transition of Polydiacetylene by Solid-State C-13 NMR. *Macromolecules* **1987**, *20*, 3094–3097.
- (23) Mitra, V. K.; Risen, W. M.; Baughman, R. H. Laser Raman Study of Stress Dependence of Vibrational Frequencies of a Monocrystalline Polydiacetylene. *J. Chem. Phys.* **1977**, *66*, 2731–2736.
- (24) Charych, D. H.; Nagy, J. O.; Spevak, W.; Bednarski, M. D. Direct Colorimetric Detection of a Receptor-Ligand Interaction by a Polymerized Bilayer Assembly. *Science* **1993**, *261*, 585–588.
- (25) Charych, D.; Cheng, Q.; Reichert, A.; Kuziemko, G.; Stroth, M.; Nagy, J. O.; Spevak, W.; Stevens, R. C. A “Litmus Test” for Molecular Recognition Using Artificial Membranes. *Chem. Biol.* **1996**, *3*, 113–120.
- (26) Okada, S.; Peng, S.; Spevak, W.; Charych, D. Color and Chromism of Polydiacetylene Vesicles. *Acc. Chem. Res.* **1998**, *31*, 229–239.
- (27) Cheng, Q.; Stevens, R. C. Coupling of an Induced Fit Enzyme to Polydiacetylene Thin Films: Colorimetric Detection of Glucose. *Adv. Mater.* **1997**, *9*, 481–483.
- (28) Huang, X.; Jiang, S. G.; Liu, M. H. Metal Ion Modulated Organization and Function of the Langmuir-Blodgett Films of Amphiphilic Diacetylene: Photopolymerization, Thermochromism, and Supramolecular Chirality. *J. Phys. Chem. B* **2005**, *109*, 114–119.
- (29) Upcher, A.; Lifshitz, Y.; Zeiri, L.; Golan, Y.; Berman, A. Effect of Metal Cations on Polydiacetylene Langmuir Films. *Langmuir* **2012**, *28*, 4248–4258.
- (30) Chanakul, A.; Traiphol, N.; Traiphol, R. Controlling the Reversible Thermochromism of Polydiacetylene/Zinc Oxide Nanocomposites by Varying Alkyl Chain Length. *J. Colloid Interface Sci.* **2013**, *389*, 106–114.
- (31) Kyeong, S.; Kang, H.; Yim, J.; Jeon, S. J.; Jeong, C. H.; Lee, Y. S.; Jun, B. H.; Kim, J. H. Quantum Dot-Assembled Nanoparticles with Polydiacetylene Supramolecule Toward Label-Free, Multiplexed Optical Detection. *J. Colloid Interface Sci.* **2013**, *394*, 44–48.
- (32) Ahn, D. J.; Chae, E. H.; Lee, G. S.; Shim, H. Y.; Chang, T. E.; Ahn, K. D.; Kim, J. M. Colorimetric Reversibility of Polydiacetylene Supramolecules Having Enhanced Hydrogen-Bonding Under Thermal and pH Stimuli. *J. Am. Chem. Soc.* **2003**, *125*, 8976–8977.
- (33) Huo, Q.; Russell, K. C.; Leblanc, R. M. Chromatic Studies of a Polymerizable Diacetylene Hydrogen Bonding Self-Assembly: A “Self-Folding” Process To Explain The Chromatic Changes of Polydiacetylenes. *Langmuir* **1999**, *15*, 3972–3980.
- (34) Wu, S.; Niu, L. F.; Shen, J.; Zhang, Q. J.; Bubeck, C. Aggregation-Induced Reversible Thermochromism of Novel Azo Chromophore-Functionalized Polydiacetylene Cylindrical Micelles. *Macromolecules* **2009**, *42*, 362–367.
- (35) Hu, W. L.; Hao, J.; Li, J. G.; Zou, G.; Zhang, Q. J. Novel Chromatic Transitions of Azobenzene-Functionalized Polydiacetylene Aggregates in 1,2-Dichlorobenzene Solution. *Macromol. Chem. Phys.* **2012**, *213*, 2582–2589.
- (36) Kim, J. M.; Lee, J. S.; Choi, H.; Sohn, D.; Ahn, D. J. Rational Design and in-Situ FTIR Analyses of Colorimetrically Reversible Polydiacetylene Supramolecules. *Macromolecules* **2005**, *38*, 9366–9376.
- (37) Jung, Y. K.; Kim, T. W.; Kim, J.; Kim, J. M.; Park, H. G. Universal Colorimetric Detection of Nucleic Acids Based on Polydiacetylene (PDA) Liposomes. *Adv. Funct. Mater.* **2008**, *18*, 701–708.
- (38) Kim, K. W.; Choi, H.; Lee, G. S.; Ahn, D. J.; Oh, M. K. Effect of Phospholipid Insertion on Arrayed Polydiacetylene Biosensors. *Colloids Surf., B* **2008**, *66*, 213–217.
- (39) Ahn, D. J.; Lee, S.; Kim, J. M. Rational Design of Conjugated Polymer Supramolecules with Tunable Colorimetric Responses. *Adv. Funct. Mater.* **2009**, *19*, 1483–1496.
- (40) Fukuda, K.; Shibasaki, Y.; Nakahara, H. Polymerizabilities of Amphiphilic Monomers with Controlled Arrangements in Langmuir-Blodgett Films. *Thin Solid Films* **1988**, *160*, 43–52.
- (41) Kaneko, F.; Shibata, M.; Kobayashi, S. Absorption Properties and Structure Changes Caused by Pre-Annealing in Polydiacetylene Langmuir-Blodgett-Films. *Thin Solid Films* **1992**, *210*, 548–550.
- (42) Britt, D. W.; Hofmann, U. G.; Mobius, D.; Hell, S. W. Influence of Substrate Properties on the Topochemical Polymerization of Diacetylene Monolayers. *Langmuir* **2001**, *17*, 3757–3765.
- (43) Jonas, U.; Shah, K.; Norvez, S.; Charych, D. H. Reversible Color Switching and Unusual Solution Polymerization of Hydrazide-Modified Diacetylene Lipids. *J. Am. Chem. Soc.* **1999**, *121*, 4580–4588.
- (44) Lifshitz, Y.; Golan, Y.; Kononov, O.; Berman, A. Structural Transitions in Polydiacetylene Langmuir Films. *Langmuir* **2009**, *25*, 4469–4477.
- (45) Mueller, A.; O'Brien, D. F. Supramolecular Materials via Polymerization of Mesophases of Hydrated Amphiphiles. *Chem. Rev.* **2002**, *102*, 727–757.
- (46) Gaboriaud, F.; Golan, R.; Volinsky, R.; Berman, A.; Jelinek, R. Organization and Structural Properties of Langmuir Films Composed

of Conjugated Polydiacetylene and Phospholipids. *Langmuir* **2001**, *17*, 3651–3657.

(47) Ma, Z. F.; Li, J. R.; Li, H.; Jiang, L. Two Dimensional Phase Separation of Diacetylenic Matrix and Glycolipids at the Air-Water Interface. *New J. Chem.* **2000**, *24*, 313–316.

(48) Lu, Y. F.; Yang, Y.; Sellinger, A.; Lu, M. C.; Huang, J. M.; Fan, H. Y.; Haddad, R.; Lopez, G.; Burns, A. R.; Sasaki, D. Y.; et al. Self-Assembly of Mesoscopically Ordered Chromatic Polydiacetylene/Silica Nanocomposites. *Nature* **2001**, *411*, 617–617.

(49) Buschl, R.; Hupfer, B.; Ringsdorf, H. Polyreactions in Oriented Systems. 30. Mixed Monolayers and Liposomes From Natural and Polymerizable Lipids. *Makromol. Chem., Rapid Commun.* **1982**, *3*, 589–596.

(50) Tyminski, P. N.; Latimer, L. H.; O'Brien, D. F. Rhodopsin in Polymerized Bilayer-Membranes. *J. Am. Chem. Soc.* **1985**, *107*, 7769–7770.

(51) Tyminski, P. N.; Latimer, L. H.; O'Brien, D. F. Reconstitution of Rhodopsin and the CGMP Cascade in Polymerized Bilayer-Membranes. *Biochemistry* **1988**, *27*, 2696–2705.

(52) Zhong, L.; Jiao, T. F.; Liu, M. H. Gemini Amphiphiles Regulated Photopolymerization of Diacetylene Acid in Organized Molecular Films. *J. Phys. Chem. B* **2009**, *113*, 8867–8871.

(53) Frankel, D. A.; Lamparski, H.; Liman, U.; O'Brien, D. F. Photoinduced Destabilization of Bilayer Vesicles. *J. Am. Chem. Soc.* **1989**, *111*, 9262–9263.

(54) Lamparski, H.; Liman, U.; Barry, J. A.; Frankel, D. A.; Ramaswami, V.; Brown, M. F.; O'Brien, D. F. Photoinduced Destabilization of Liposomes. *Biochemistry* **1992**, *31*, 685–694.

(55) Vollhardt, D.; Liu, F.; Rudert, R. The Role of Nonsurface-Active Species at Interfacial Molecular Recognition by Melamine-Type Monolayers. *J. Phys. Chem. B* **2005**, *109*, 17635–17643.

(56) Giner-Casares, J. J.; de Miguel, G.; Perez-Morales, M.; Martin-Romero, M. T.; Camacho, L.; Munoz, E. Effect of the Molecular Methylene Blue Aggregation on the Mesoscopic Domain Morphology in Mixed Monolayers with Dimyristoyl-Phosphatidic Acid. *J. Phys. Chem. C* **2009**, *113*, 5711–5720.

(57) Gonzalez-Delgado, A. M.; Rubia-Paya, C.; Roldan-Carmona, C.; Giner-Casares, J. J.; Perez-Morales, M.; Munoz, E.; Martin-Romero, M. T.; Camacho, L.; Brezesinski, G. Control of the Lateral Organization in Langmuir Mono layers via Molecular Aggregation of Dyes. *J. Phys. Chem. C* **2010**, *114*, 16685–16695.

(58) Gonzalez-Delgado, A. M.; Giner-Casares, J. J.; Rubia-Paya, C.; Perez-Morales, M.; Martin-Romero, M. T.; Brezesinski, G.; Camacho, L. The Effect of the Reduction of the Available Surface Area on the Hemicyanine Aggregation in Laterally Organized Langmuir Monolayers. *J. Phys. Chem. C* **2011**, *115*, 9059–9067.

(59) Scheibe, P.; Schoenhentz, J.; Platen, T.; Hoffmann-Roder, A.; Zentel, R. Langmuir-Blodgett Films of Fluorinated Glycolipids and Polymerizable Lipids and Their Phase Separating Behavior. *Langmuir* **2010**, *26*, 18246–18255.

(60) Gruniger, H.; Mobius, D.; Meyer, H. Enhanced Light-Reflection by Dye Monolayers at the Air-Water-Interface. *J. Chem. Phys.* **1983**, *79*, 3701–3710.

(61) Buffeteau, T.; Desbat, B.; Turlet, J. M. Polarization Modulation FTIR Spectroscopy of Surfaces and Ultra Thin Films. Experimental Procedure and Quantitative Analysis. *Appl. Spectrosc.* **1991**, *45*, 380–389.

(62) Hada, H.; Hanawa, R.; Haraguchi, A.; Yonezawa, Y. Preparation of the J-Aggregate of Cyanine Dyes by Means of the Langmuir-Blodgett Technique. *J. Phys. Chem.* **1985**, *89*, 560–562.

(63) Yonezawa, Y.; Mobius, D.; Kuhn, H. Scheibe-Aggregate Monolayers of Cyanine Dyes without Long Alkyl Chains. *Ber. Bunsenges. Phys. Chem* **1986**, *90*, 1183–1188.

(64) Young, M. C. J.; Jones, R.; Tredgold, R. H.; Lu, W. X.; Aliadib, Z.; Hodge, P.; Abbasi, F. Optical and Structural Characterization of Langmuir-Blodgett Multilayers of Non-Polymeric and Polymeric Hemicyanines. *Thin Solid Films* **1989**, *182*, 319–332.

(65) Hall, R. A.; Thistlethwaite, P. J.; Grieser, F.; Kimizuka, N.; Kunitake, T. The Formation and Structure of Aggregates in Hemicyanine Monolayers. *Colloids Surf., A* **1995**, *103*, 167–172.

(66) Goettgens, B. M.; Tillmann, R. W.; Radmacher, M.; Gaub, H. E. Molecular Order in Polymerizable Langmuir-Blodgett-Films Probed by Microfluorescence and Scanning Force Microscopy. *Langmuir* **1992**, *8*, 1768–1774.

(67) Turshatov, A. A.; Mobius, D.; Bossi, M. L.; Hell, S. W.; Vedernikov, A. I.; Lobova, N. A.; Gromov, S. P.; Alifimov, M. V.; Zaitsev, S. Y. Molecular Organization of an Amphiphilic Styryl Pyridinium Dye in Monolayers at the Air/Water Interface in the Presence of Various Anions. *Langmuir* **2006**, *22*, 1571–1579.

(68) Roldan-Carmona, C.; Giner-Casares, J. J.; Perez-Morales, M.; Martin-Romero, M. T.; Camacho, L. Revisiting the Brewster Angle Microscopy: The relevance of the polar headgroup. *Adv. Colloid Interface Sci.* **2012**, *173*, 12–22.

(69) Volinsky, R.; Gaboriaud, F.; Berman, A.; Jelinek, R. Morphology and Organization of Phospholipid/Diacetylene Langmuir Films Studied by Brewster Angle Microscopy and Fluorescence Microscopy. *J. Phys. Chem. B* **2002**, *106*, 9231–9236.

(70) Gaboriaud, F.; Volinsky, R.; Berman, A.; Jelinek, R. Temperature Dependence of the Organization and Molecular Interactions within Phospholipid/Diacetylene Langmuir Films. *J. Colloid Interface Sci.* **2005**, *287*, 191–197.

(71) Rideal, D. *Interfacial Phenomena*; Academic Press: London, 1963; pp 217–281.

(72) Pedrosa, J. M.; Romero, M. T. M.; Camacho, L.; Mobius, D. Organization of an Amphiphilic Azobenzene Derivative in Monolayers at the Air-Water Interface. *J. Phys. Chem. B* **2002**, *106*, 2583–2591.

(73) Song, Q.; Evens, C. E.; Bohn, P. W. Spectroscopic Characterization of Aggregation Behavior in Hemicyanine Dye Monolayer and Multilayer Systems. *J. Phys. Chem.* **1993**, *97*, 13736–13741.

(74) Lusk, A. L.; Bohn, P. W. Spatial and Spectral Heterogeneity in Fluorescence From Monolayers if 4-(4-(Di-hexadecylamino)Styryl)-N-Methylpyridinium Iodide. *Langmuir* **2000**, *16*, 9131–9136.

(75) Lusk, A. L.; Bohn, P. W. Effect of Processing Conditions on the Formation of Aggregates and Phase Domains in Monolayers of the Hemicyanine Dye, 4-(4-(Di-hexadecylamino)Styryl)-N-Methylpyridinium Iodide. *J. Phys. Chem. B* **2001**, *105*, 462–470.

(76) Tachibana, H.; Yamanaka, Y.; Sakai, H.; Abe, M.; Matsumoto, M. In Situ AFM Study on the Morphological Change of the Langmuir-Blodgett Film of Cadmium 10,12-Pentacosadiynoate during Polymerization. *Langmuir* **2000**, *16*, 2975–2977.

(77) Mino, N.; Tamura, H.; Ogawa, K. Photoreactivity of 10,12-Pentacosadiynoic Acid Monolayers and Color Transitions of the Polymerized Monolayers on an Aqueous Subphase. *Langmuir* **1992**, *8*, 594–598.

(78) Davydov, A. S. *Theory of Molecular Excitons*; McGraw-Hill: New York, 1962.

(79) Pope, M.; Swenberg, C. E. *Electronic Processes in Organic Crystals and Polymers*; Oxford Science Publications: New York, 1999; pp 39–89.

(80) Carpick, R. W.; Sasaki, D. Y.; Burns, A. R. First Observation of Mechanochromism at the Nanometer Scale. *Langmuir* **2000**, *16*, 1270–1278.

(81) Ryu, S.; Yoo, I.; Song, S.; Yoon, B.; Kim, J. M. A Thermoresponsive Fluorogenic Conjugated Polymer for a Temperature Sensor in Microfluidic Devices. *J. Am. Chem. Soc.* **2009**, *131*, 3800–3801.

(82) Fernandez, A. J.; Ruiz, J. J.; Camacho, L.; Martin, M. T.; Munoz, E. Orientation and Organization of Langmuir-Blodgett Mixed Films Consisting of a Phospholipid and a Viologen Studied by Infrared Spectroscopy. *J. Phys. Chem. B* **2000**, *104*, 5573–5578.

(83) Gao, W.; Dickinson, L.; Grozinger, C.; Morin, F. G.; Reven, L. Self-Assembled Monolayers of Alkylphosphonic Acids on Metal Oxides. *Langmuir* **1996**, *12*, 6429–6435.

(84) Lozano, P.; Fernandez, A. J.; Ruiz, J. J.; Camacho, L.; Martin, M. T.; Munoz, E. Molecular Organization of LB Multilayers of

Phospholipid and Mixed Phospholipid/Viologen by FTIR Spectroscopy. *J. Phys. Chem. B* **2002**, *106*, 6507–6514.

(85) Sinniah, K.; Cheng, J.; Terrettaz, S.; Reutt-Robey, J. E.; Miller, C. J. Self-Assembled Omega-Hydroxyalkanethiol Monolayers with Internal Functionalities: Electrochemical and Infrared Structural Characterizations of Ether Containing Monolayers. *J. Phys. Chem.* **1995**, *99*, 14500–14505.

(86) Snyder, R. G.; Maroncelli, M.; Strauss, H. L.; Hallmark, V. M. Temperature and Phase Behavior of Infrared Intensities: The Poly(Methylene) Chain. *J. Phys. Chem.* **1986**, *90*, 5623–5630.

(87) Snyder, R. G.; Strauss, H. L.; Elliger, C. A. Carbon-Hydrogen Stretching Modes and the Structure of N-Alkyl Chains. 1. Long, Disordered Chains. *J. Phys. Chem.* **1982**, *86*, 5145–5150.

(88) Gericke, A.; Huhnerfuss, H. In-Situ Investigation of Saturated Long-Chain Fatty-Acids at the Air-Water Interface by External Infrared Reflection-Absorption Spectrometry. *J. Phys. Chem.* **1993**, *97*, 12899–12908.

(89) Gericke, A.; Huhnerfuss, H. Investigation of Z-Unsaturated and E-Unsaturated Fatty-Acids, Fatty-Acid Esters, and Fatty Alcohols at the Air-Water-Interface by Infrared-Spectroscopy. *Langmuir* **1995**, *11*, 225–230.

(90) de Miguel, G.; Pedrosa, J. M.; Martin-Romero, M. T.; Munoz, E.; Richardson, T. H.; Camacho, L. Conformational Changes of a Calix[8] Arene Derivative at the Air-Water Interface. *J. Phys. Chem. B* **2005**, *109*, 3998–4006.

(91) Su, Y. L.; Li, J. R.; Jiang, L. Effect of Amphiphilic Molecules Upon Chromatic Transitions of Polydiacetylene Vesicles in Aqueous Solutions. *Colloids Surf., B* **2004**, *39*, 113–118.

(92) Su, Y. L.; Li, J. R.; Jiang, L. A Study on the Interactions of Surfactants with Phospholipid/Polydiacetylene Vesicles in Aqueous Solutions. *Colloids Surf., A* **2005**, *257–58*, 25–30.